Peptides 152 (2022) 170760

Contents lists available at ScienceDirect

Peptides

journal homepage: www.elsevier.com/locate/peptides

Albumin binding Nanofitins, a new scaffold to extend half-life of biologics – a case study with exenatide peptide

Nadine Michot [a,1], Aurélia Guyochin [a,1], Mathieu Cinier [d,1,*], Chloé Savignard [d], Olivier Kitten [d], Marie-Hélène Pascual [b], Stéphanie Pouzieux [c], Marie-Laure Ozoux [b], Patrick Verdier [b], Pascale Vicat [b], Jacques Dumas [a]

[a] Sanofi, Biologics Research, Vitry sur Seine, 94430, France
[b] Sanofi, Drug Safety & Animal Research, Alfortville 94430, France
[c] Sanofi, Integrated Drug Discovery, Vitry sur Seine, 94430, France
[d] Affilogic, Nantes 44200, France

ARTICLE INFO

Keywords:
Exenatide
Nanofitin
Albumin
ABNF
Half-life extension

ABSTRACT

A new strategy of peptide half-life extension has been evaluated. We investigated libraries of a small and very stable protein scaffold called Nanofitin, capable of high affinity for protein targets. We have identified Nanofitins targeting Human and mouse Serum Albumin, which could significantly improve the pharmacokinetics of an active associated peptide, mobilizing the patient's own albumin without external source. To demonstrate the impact of this approach on half-life extension, a genetic fusion of an Exenatide peptide with an Albumin Binding Nanofitin (ABNF) was performed. Specific activity of Exenatide-ABNF was measured and unaffected by the fusion. In vivo mice results provided convincing data (t½ of 8 min for Exenatide peptide compared to 20 h for Exenatide-ABNF) with sustained pharmacological activity over 3 days. This study constitutes a proof-of-concept of in vivo half-life extension of a biologic using an ABNF. Besides, the absence of cysteine in the Nanofitin scaffold, which is therefore devoid of structuring disulfide bonds, allows manufacturing in microbial cost effective systems.

1. Introduction

Peptides and small proteins generally exhibit a short plasma half-life which limits their therapeutic use. This can be attributed in part to a rapid renal clearance. The serum half-life of proteins smaller than 70 kDa, generally admitted as the glomerular filtration cutoff, has been reported to be less than one hour [1,2]. Different strategies have been developed to address this pharmacokinetic issue The chemical or genetic fusion to large artificial or natural macromolecules, such as polyethylene glycol [1,2], XTEN polypeptide [3,4], human serum albumin (HSA) [5] and albumin binding proteins [6] are well described technological solutions to limit renal clearance. While the first two rely on the increase of the hydrodynamic radius of the molecule of interest, the last two aim at diverting the natural FcRn dependent recycling of the albumin for the benefit of half-life extension [7]. Having a range of solutions at disposal is critical when considering a given molecule, as they can show different tolerance profiles to one or another, both from a conjugation and functionality standpoints.

A good example of that is provided by the case of Exenatide. Exenatide is a 39-amino acid glucagon-like peptide-1 receptor (GLP1-R) agonist indicated for the treatment of type 2 diabetes mellitus as subcutaneous injection twice daily [8,9,10]. It has a short plasma half-life of 2.4 h and an action time of about 8 h [11]. As is known, daily injection is associated with complication such as infection at the sites of injection and poor patient compliance. Moreover, the fluctuation of drug plasma concentration may also aggravate side effects such as sour stomach, diarrhea, heartburn, indigestion, belching, nausea, and vomiting [11]. Long lasting Exenatide would allow to widen the time between two injections and facilitate type 2 diabete patients' care and compliance to treatment [12]. Genetic fusion or chemical conjugation of Exenatide to

Abbreviations: ABNF, albumin binding Nanofitin.

* Corresponding author.
E-mail address: mathieu@affilogic.com (M. Cinier).

[1] These authors contributed equally to this work

https://doi.org/10.1016/j.peptides.2022.170760
Received 9 December 2021; Received in revised form 3 February 2022; Accepted 7 February 2022
Available online 9 February 2022

albumin [13], PEG [14,15] and 864-amino acid long XTEN polypeptide [16] have already been described. All resulted in a significant increase of the plasma half-life (from 8 min to ~12–38 h in mice), to the expense of a decrease of the activity of the cargo peptide. We hypothetized that albumin binding technologies based on small protein scaffolds and allowing a reversible, non-covalent association with the serum protein could provide similar half-life increase with minimal impact on the activity of the cargo by limiting the steric hindrance at the anchoring point [17,18].

Nanofitins are small (7 kDa) alternative binding proteins derived from the naturally hyperthermostable Sac7d protein found in *Sulfulobus acidocaldarius* [19,20]. They are single chain, 66 amino acids long, lack cysteine, and are spontaneously folded during the expression in microorganisms. Protein engineering efforts have allowed the identification of suitable positions that can be randomized to generate Nanofitins libraries, making then possible to isolate Nanofitins of high affinity and specificity for a protein target [20–29]. They are tolerant to fusion either at the N- or C-terminus and offer unique physico-chemical properties to streamline product development [26]. Their extreme resistances to high temperature (above 80 °C) [20,26] and extreme pH (pH 1–13) [23] are key assets, notably in term of manufacturing and formulation perspectives, for their positioning as therapeutic ingredient. This positioning shall be further consolidated along with the development of the Nanofitin technology and other alternative scaffolds in the therapeutic space, notably with regard to immunogenicity concern. In this work, we are describing the generation of a high affinity albumin binding Nanofitin (ABNF) and demonstrating its half-life extension potential in a proof-of-concept study using Exenatide as a model cargo. Our preclinical data showed that the anti-albumin Nanofitin fusion dramatically increased the plasma half-life of Exenatide without impairing its biological activity, which results in a sustained control of blood glucose level for more than 3 days.

2. Materials and methods

2.1. Binding kinetics of the ABNF on HSA and MSA

The procedures for the selection of the ABNF by ribosome display, the identification of the ABNF and its recombinant production are described in the supplementary material. Binding kinetic parameters of the ABNF on HSA and MSA were measured by biolayer interferometry on Octet RED96 system (FortéBio). Biotinylated HSA and MSA were diluted to 0.5 μg/mL and loaded on streptavidin biosensors at 1 nm, then biosensors were allowed to equilibrate for 60 s. Binding kinetic was then evaluated by exposing simultaneously biosensors to a concentration range of the ABNF (from 15.6 to 1000 nM). Association and dissociation steps were measured for 180 s each. All steps were performed in TBS containing 0.002% Tween 20% and 0.01% Protein Free Blocking Buffer. Biosensors were regenerated using three cycles of alternating wash for 10 s in Glycine 10 mM pH 2.5 and in TBS. All the steps were run at 30 °C with a continuous shake speed of 1000 RPM. For each set of measurement, one biosensor exposed to the 0 nM concentration was used as a background reference. Sensorgrams were processed using a single reference subtraction and analyzed using the Octet Data Analysis software HT 11.1 (FortéBio). Fitting was performed with a 1:1 binding fit model.

2.2. Binding of the ABNF on HSA domains I, II and III

HSA domains I, II and III were obtained from Albumin Bioscience and biotinylated with Sulfo-NHS-LC-LC-Biotin (Pierce) according to the manufactured instructions. ELISA was performed on streptavidin plate using Protein Free Blocking Buffer (Pierce) as blocking solution. Biotinylated HSA domains (100 μL, 40 nM) in Protein Free Blocking Buffer were immobilized for 1 h at RT with shaking. Prior all the following incubation steps, the wells were washed 3 times with TBS with 0.1% Tween 20. The ABNF (100 nM) was applied to wells for 1 h at RT with shaking. Revelation was then carried over by the addition of 100 μL of RGS His antibody HRP conjugate (Qiagen) diluted 1/4000 in TBS with 0.1% Tween 20 for 1 h at RT with shaking, followed by the addition of 100 μL of a 10 mg/mL solution of 3,3′,5,5′-tetramethylbenzidine substrate (Merck) in revelation buffer (0.1 M Citrate/acetate buffer pH 6, 1.2% hydrogen peroxide). The reaction was stopped by the addition of 1 M HCl (100 μL/well) and absorbance at 450 nm was measured using an ELISA plate reader (Varioskan).

2.3. Plasmid constructs and expression of fusion proteins

DNA constructions for the expression of recombinant Exenatide and Exenatide-ABNF fusions were obtained by gene synthesis (GeneArt) with codon optimization for E.coli expression. In all the case Exenatide has been fused at the N-terminus with a hexahistidine and a SUMO tags. In addition, all constructs contained a cleavage site for TEV protease (ENLYFQ/H instead of ENLYFQ/GS, the canonical recognition site) after the His-SUMO tag to facilitate the proper removal of the fusion tags upon purification. For the exenatide-ABNF fusions, different linkers in term of length and amino acids composition were investigated. All products were subcloned into the *Nde*I and *Not*I restriction sites of the pET29a vector. The fusion proteins were expressed in E.coli BL21 (DE3) strain. Five hundred milliliters of 2YT, 2% glucose and kanamycin (50 mg/L) were inoculated with 50 mL of overnight pre-culture of transformed BL21 (DE3) and grown to exponential phase at 28 °C. Then, the culture with determined volume to be at 1 OD/mL was auto-induced overnight at 20 °C in one liter of ZYM-5052 growth media. Cells were harvested by centrifugation.

2.4. Purification of fusion proteins

Cells were resuspended in 200 mL of PBS 3x containing 35 mM imidazole, 0.1% Triton X-100, protease inhibitor cocktail EDTA free (Roche) and nuclease. After addition of 100 mg of lysozyme, cells were incubated for 1 h at 4 °C. The bacterial lysate was centrifuged at 10 000 g for 1 h at 4 °C to remove the insoluble fraction. Supernatant containing soluble proteins was recolted. The bacterial supernatant was loaded onto a His Trap HP (GE Healthcare) column equilibrated with PBS 3x, 35 mM imidazole and 0.1% Triton X-100. After a first washing step (PBS 3x, 35 mM imidazole, 0.1% Triton X-100) to remove endotoxins and a second one (PBS 3x, 35 mM imidazole), the His-SUMO tagged fusion proteins were eluted with PBS 3x, 300 mM imidazole. Protein concentration was determined by A280 and calculated using the extinction coefficient of each protein. After that, proteins were dialyzed overnight against PBS 3x, 35 mM imidazole and TEV protease to remove His-SUMO tag at the N-ter of the fusion protein.

Fusion proteins were loaded again onto a His Trap HP column, in negative way. Proteins of interest were retrieved in the flow though without contaminants. Protein fractions were pooled, dialyzed against PBS 1x, concentrated by Vivaspin (MWCO: 3000) and filtered using a 0.22 μm filter. The final concentration of purified fusion proteins was determined by A280. Reverse phase high performance liquid chromatography coupled with mass spectrometry using Electrospray ionization (LC-MS) was performed to confirm the identity of the purified fusion proteins. The Kinetic-QCLTM assay was performed to evaluate the presence of Gram negative bacteria endotoxin. Protein samples were mixed with the Limulus Amebocyte Lysate (LAL)/substrate reagent, placed in an incubating plate reader and monitored for the appearance of a yellow color. Sensitivity range was between 0.005 EU/mL and 50.0 EU/mL.

2.5. Characterization of fusion proteins by SEC and nanoDSF

Determination of protein homogeneity after purification under native condition (50 mM Tris, 150 mM NaCl, pH 7.5) and estimation of

molecular size was accomplished through size exclusion chromatography using a Superdex 200 increase 5/150 (GE Healthcare). For the thermal stability, the proteins were diluted to a final concentration of 10 μM. Then, fusion proteins solutions were loaded into nanoDSF grade capillaries (NanoTemper Technology) and loaded into the Prometheus NT.48 instrument. The temperature gradient was set to an increase of 1 °C/min in a range from 20 °C to 90 °C. Protein unfolding was measured by detecting the temperature dependent change in tryptophan fluorescence at emission wavelengths of 330 and 350 nm. Melting temperatures were determined automatically from the second derivative of the fluorescence ratio (F350/F330).

2.6. Binding kinetic of the Exenatide-ABNF fusion on HSA and MSA at pH 7.4 and 6

Experiments were performed by biolayer interferometry (Octet Qke, Fortébio). 100 nM of biotinylated albumin were loaded to streptavidin biosensors. Binding curves were generated by the association (300 s)/dissociation (1800 s) of fusion proteins diluted over a range of concentrations from 1.5 to 100 nM in assay diluent. For experiments at pH 7.4 and pH 6, assay diluent was respectively HBS-EP pH 7.4 supplemented with 0.05% Tween20 and PBS 1x pH 6.0. Before each measurement, a baseline was measured, which was subtracted from the binding curve. Affinity (KD) was calculated by fitting on-rate and off-rate curves using the Octet software.

2.7. In vitro functional GLP1R cell based assay

Fusion proteins were tested in agonist mode in the classical in vitro GLP1R cell based assay based on cAMP measurements (DiscoverX). Samples were assayed in duplicate over a ten concentration points using three fold serial dilution of a solution at 50 nM. Each sample was tested in presence and absence of six molar equivalent of MSA, to investigate its influence on the dose response. Data was normalized to the maximal and minimal response observed in the presence of control ligand (Exendin-4) and vehicle. EC50 was determined by interpolation of the fitted data using GraphPad Prism V6.01.

2.8. In vivo assays: pharmacokinetics and in vivo glucose tolerance test

Male CD1 mice (6 or 7 weeks old) from Charles River Laboratories (Italia SRL) were used in the current studies. All mice were maintained under 12-hour light/dark cycle with free access to food and water. All experiments were conducted in compliance with federal guidelines or recommendations.

For pharmacokinetic studies, CD1 mice (male, 6–7 weeks, weight between 25 and 30 g, 3 mice per time-point and 6 mice per group) received an intravenous injection of 250 μL of the fusion proteins at 0.5 mg/mL. In time intervals of 0.083, 0.5, 4, 24, 48 and 72 h, blood samples (100 μL) were collected from the tail and incubated on ice. Heparinized blood samples were centrifuged at 1500 g for 10 min at 4 °C in order to obtain plasma and samples were stored at − 80 °C until analysis. Plasma concentration of fusion proteins were determined by ELISA. The assay was based on the capture of Exenatide or Exenatide-ABNF by a polyclonal rabbit anti-Exenatide antibody and its recognition by a monoclonal mouse anti-Exenatide antibody (kit ABBiolabs, ref-SEK 0130–01). Measurements were made by the reading of TMB oxidized product (visible detection at 450 nm / correction at 620 nm) within 30 min. Raw data (OD) measured by the plate reader were plotted against nominal standard concentrations deduced from the respective standard calibration curves established for each of the different Exenatide-ABNF contructs. Half-life (t1/2 z), AUC and CL were determined.

For the oral glucose tolerance test (OGTT), two of the Exenatide-ABNF fusions were investigated (Exenatide-12aa-ABNF and Exenatide-Exenatide-4aa-ABNF) in a side by side comparison with Exenatide and vehicule only (PBS). At day 1, the test items (200 nmol/kg) were administered to the mice by i.v. infusion right after a measurement of their blood glucose level. Fifteen minutes after the infusion, an oral glucose load of 2 g/kg (40 mL/kg) was given and the blood glucose levels were measured at 0.25, 0.5, 1, 2, and 4 h after the glucose administration. At days 2 and 3, the baseline glucose level was first measured, corresponding at 24 h and 48 h after the infusion of the test items, and 15 min after mice were challenged with an oral glucose load again. Blood glucose levels were measured at 1, 2, and 4 h after glucose challenge. Blood glucose levels (mg/dl) were determined using a glucometer (Accu-Chek Performa). One whole blood drop taken in the saphenous vein of mice was absorbed by a test trip. Data was entered in Provantis software after conversion in mmol/l. The level of statistical significance was $p \leq 0.05$.

3. Results and discussion

3.1. Selection of albumin binding Nanofitins (ABNF) by ribosome display

Nanofitin libraries were challenged against human serum albumin in four panning rounds by ribosome display. Enrichment toward albumin binders resulted in the isolation of 9 different Nanofitins that could be grouped into four families of sequences based on their respective homologies. Initial characterization was performed using supernatants from micro-culture to screen for their ability at cross reacting between the human and mouse serum albumins (Fig. S1A). The cross reactivity was set as a prerequisite to support preclinical demonstration in mouse models and allowed to narrow down our interest to three Nanofitins (NF1, NF4 and NF9). Comparison of their binding efficiency on human serum albumin in ELISA over a range of three concentrations (62.5, 250 and 1000 nM) clearly highlighted the higher binding capacity of NF1 (Fig. S1B), which was then chosen as the albumin binding Nanofitin (ABNF) to focus on in the study. Preliminary evaluation of its affinity at pH 7.4 on human and mouse serum albumins by biolayer interferometry resulted in KD of 0.11 nM and 13 nM respectively (Fig. 1). The isolation of Nanofitins displaying subnanomolar affinity for their target straight out of the panning campaign was already reported by Mouratou et al. [20]. The potential at delivering high affinity binders is a key asset of the Nanofitin technology as a druggable alternative scaffold.

The albumin is composed of three domains (I, II and III), with the domains I and III being involved in its interaction with FcRn (Fig. 1D). FcRn protects albumin from intracellular degradation via a pH-dependent cellular recycling mechanism, which contributes to its long half-life of about 3 weeks in human. To get insight on the ABNF mode of interaction with albumins, we evaluated in ELISA its ability at binding the different domains of HSA using commercially available recombinant versions of domains I (1−197), II (189−385) and III (381−585). It has been reported that the three domains can fold independently and exhibit secondary and tertiary structure similar to that of HSA[30].

The ABNF was found able to bind only the domain II (Fig. 1C), which happens to be spatially distant from the FcRn interaction site (Fig. 1D). Albumin binding domains derived from Streptococcal protein G have been widely described for their ability at promoting half-life extension to cargo molecules [6,31]. Interestingly, they were also described to target the domain II of albumin [32] and found not to interfere with the Albumin/FcRn interaction in vivo [33], resulting in a prolonged residence in the blood stream despite of their low molecular weight (5 kDa). The high affinity of the ABNF and its binding location at the domain II of HSA, are both suggesting that the ABNF could sustain a prolonged serum half-life in vivo and be used as a half-life extension module. For the demonstration, we set a therapeutically oriented proof-of-concept study involving Exenatide-ABNF fusion constructions.

3.2. Production and characterization of Exenatide-ABNF fusion proteins

Exenatide requires a free N-terminal histidine to be fully functional [34]. The recombinant production of Exenatide was performed using a

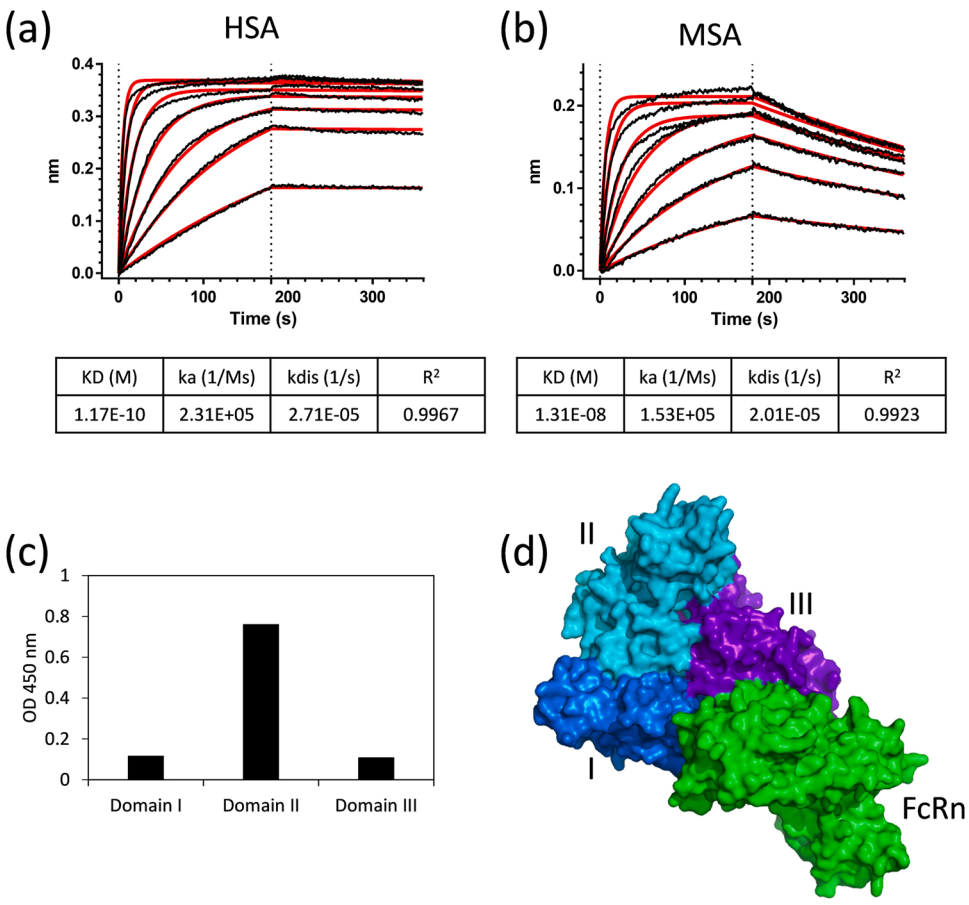

KD (M)	ka (1/Ms)	kdis (1/s)	R^2
1.17E-10	2.31E+05	2.71E-05	0.9967

KD (M)	ka (1/Ms)	kdis (1/s)	R^2
1.31E-08	1.53E+05	2.01E-05	0.9923

Fig. 1. Affinity, cross-reactivity and epitope mapping of the ABNF. (a, b): Affinity measurement by interferometry of the ABNF on HSA and MSA. Kinetic characterization was performed over a range of concentration from 15.6 to 1000 nM. Black curves represent experimental data and grey curves represent the statistical fitting of the curves. (c): evaluation of the binding of the ABNF on domain I, II and II of the HSA by ELISA. (d): Surface representation of the HSA/FcRn complex. The FcRn, the HSA domains I, II and III are respectively labelled in green, blue, cyan and purple. (For interpretation of the references to colour in this figure legend, the reader is referred to the web version of this article.)

chimeric construction with an N-terminal SUMO tag that is linked to the Exenatide peptide by a modified Tobacco etch virus (TEV) protease cleavage sequence (ENLYQ/H). The canonical TEV cleavage sequence ENLYQ/(G/S) leaves a residual G/S residue at the N-terminal end upon TEV cleavage. Although glycine and serine are conventionally described as the preferred residues at the P1' site of the TEV cleavage motif, Kapust et al. demonstrated that histidine is also very well tolerated at this position [35]. Accordingly, we modified the TEV cleavage sequence to ENLYQ/H to allow the release of Exenatide with its native N-terminal Histidine. Exenatide-ABNF fusions were prepared starting from the same chimeric construction. In all the cases, the ABNF was fused to the C-terminus of Exenatide using a linker in between to limit potential undesirable outcomes such as misfolding of the fusion protein or low yield of protein production. In this regard, linkers of different length and composition (4, 7, 12 and 25 amino acids) were explored, using the IEGR motif (Factor Xa protease recognition site [36]), the ASTKGPS motif (found at the Ntermini of human CH1 domain [37]) and glycin-rich stretches [38] (Fig. 2). We also investigated a longer linker insertion with the head to tail fusion of two Exenatide peptides flanked with the IEGR motif at the C-terminus end. In this construction, the second Exenatide peptide sequence is used as a spacer as well. Such a design with a tandem insertion of GLP-1R agonist was already described for the engineering of Albugon, which is approved for the treatment of type 2 diabetes in adults since 2014 [39].

Exenatide-ABNF fusion proteins were expressed at high level (> 60 mg/L) in E. coli cytoplasm in standard low density small scale cultures. No detectable material was found in the insoluble fraction.

N-terminal sequencing confirmed the correct processing of the fusion showing the native histidine at the N-terminal end. Quality control of the preparations included the confirmation of a low endotoxin level for in vivo testing. Endotoxin level was assayed using the FDA-approved

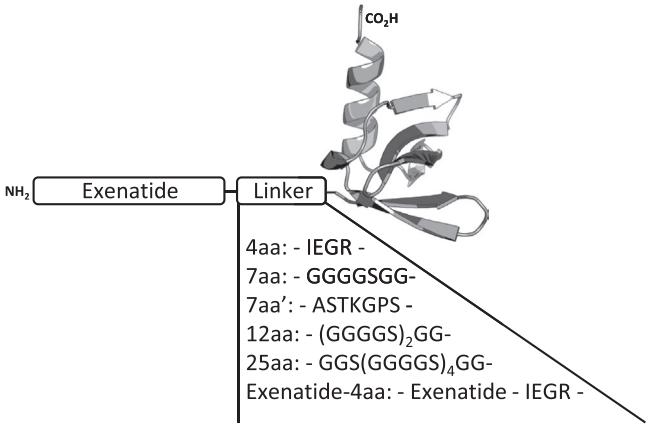

Fig. 2. Scheme of the different Exenatide-ABNF fusions and sequences of the different linkers. The representation of the Nanofitin is based on the PDB file 1AZP.

Limulus Amoebocyte Lysate (LAL) and found to be as low as < 1 endotoxin units/mg of protein. The absence of cysteine in the Nanofitin scaffold, which is therefore devoid of structuring disulfide bonds, allows its manufacturing as a soluble protein in microbial cost effective systems. This offers a true advantage in a very competitive environment.

Thermal denaturation experiments performed by nanoDSF (Prometheus, Nanotemper) revealed a Tm of 54 °C for Exenatide alone (Fig. 3A). The Exenatide-4aa-ABNF shows a Tm above 85 °C in a similar setting (Fig. 3B). The Tm could not be clearly measured for the latter as the plateau was still not reached at a temperature as high as at 95 °C. Further characterization by size exclusion chromatography revealed

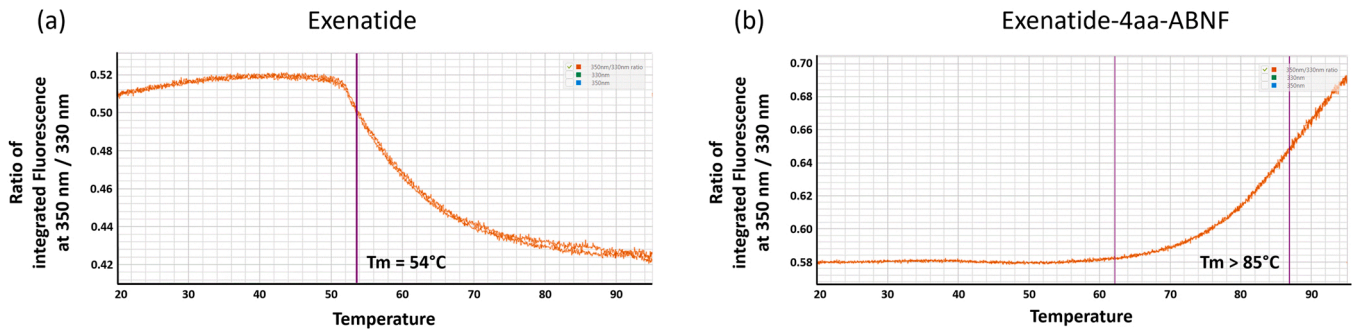

Fig. 3. Thermal denaturation profiles of Exenatide (a) and Exenatide-4aa-ABNF fusion (b) by nanoDSF.

heterogeneity in the recombinant Exenatide preparation, whereas the Exenatide-4aa-ABNF fusion was found homogeneous under the form of a single symmetric peak (Fig. S2). The source of heterogeneity observed with the Exenatide preparation has not been investigated. A similar profile of thermal denaturation and size exclusion chromatography to that of Exenatide-4aa-ABNF was observed for the other exenatide-ABNF fusions (Data not shown). These results are reflecting the extreme stability of the Nanofitin scaffold and suggest that fusing the ABNF to Exenatide stabilizes the peptide.

3.3. *In vitro binding and biological activity of Exenatide-ABNF fusions*

Functionality conservation of the ABNF when fused to Exenatide was investigated by biolayer interferometry. We evaluated the binding kinetic of the two constructions involving the shortest and longest linker length, respectively Exenatide-4aa-ABNF and Exenatide-Exenatide-4aa-ABNF. The measurements were performed both at pH 7.4 and pH 6 and compared to the data obtained for the ABNF alone in the same experimental conditions. Overall, the two chimeric constructions displayed similar affinities than the isolated ABNF on both serum albumins (Fig. 4), suggesting that the fusion do not impair the functionality of the Nanofitin. Small deviations are observed on the association rate, which appears to be slowed down when the ABNF is fused to Exenatide.

Such effect is commonly observed when fusing a protein with an unstructured polypeptide [40,41]. Even though GLP-1 and derivatives are not described as unstructured [42], the labile region created by the insertion of the linker might act as such. We observed that the ABNF displays a higher affinity at pH 6 than pH 7.4. Interestingly, this effect appears to be more pronounced on the MSA than on the HSA. A tight binding at pH 6 is a key feature for the ABNF which has to remain bound to the albumin during FcRN mediated recycling of the albumin to provide an efficient plasma half-life extension [7].

Assessment of the functionality of Exenatide in the chimeric constructions was performed in the classical in vitro GLP1R cell based assay based on cAMP measurements (Fig. 5). To generate information that reflects as much as possible the in vivo situation, the evaluation was also performed in presence of MSA (Figure SI2). All the constructions were found highly potent in the GLP1R based assay, with EC50 ranging from 0.37 nM to 1.39 nM for the chimeric constructions and of 0.43 nM for the Exenatide alone (Fig. 5). Although all the EC50 measured were in the same order of magnitude, it is interesting to note that the highest EC50 was found with the shortest linker length (Exenatide-4aa-ABNF) and the lowest EC50 with the longest (Exenatide-Exenatide-4aa-ABNF).

In a similar cell based assay, Baggio et al. compared the potency of Exendin-4 with Albugon (also known as Albiglutide), which consist in a tandem repeat of a DPPIV-resistant derivative of the GLP-1 peptide fused at the N-terminus of HSA [13]. In their study, the HSA conjugate was found with a hundred-fold lower potency than Exendin-4 alone, which they attributed to a potential steric hindrance of the HSA moiety. This is consistent with other finding made by Gong et al. in their evaluation of the impact of PEGylation on the potency of an Exenatide variant, using PEG chains of various length (5, 20, 30 and 40 kDa). They reported a drop in the potency only when using PEG chain of 30 kDa and above, suggesting a deleterious effect of a bulky conjugate as well [14]. Interestingly, the fusion of an Exenatide variant using a GSS linker with the small albumin binding domain (ABD035, 5 kDa) also resulted in a drop in activity of hundred fold in a GLP1 receptor functionality assay compared to Exenatide variant alone [43]. This latter study suggests that loss of activity of the cargo peptide cannot be rationalized only based on the bulkiness of the conjugate. In line with this observation, Kim et al. recently reported a loss of activity of a GLP-1 derivative when fused to a novel HSA binder based on the repebody scaffold using a rigid helical linker [44]. In all of these studies, the loss of activity was largely compensated in vivo by the longer residence of the molecule in the blood stream compared to the reference Exenatide. It also provides the evidence that all the half-life extension strategies might not be equivalent at maintaining a given cargo molecule in its functional state. The nature of the half-life extension modules and their respective structural constraints might be of importance too, which in this case provide a good demonstration of the ABNF potential as a therapeutic ingredient. Negligible variation of the potency was found when conjugating Exenatide with the ABNF with a variety of linker length and composition.

3.4. *In vivo functionality assessment*

We confirmed the half-life extension potential of the ABNF in a pharmacokinetic study in mice. The fusion proteins were administrated intravenously and their plasma concentration were measured by ELISA at different time points. While the Exenatide alone displays a plasma half-life less than 5 min, fusion of the peptide with the ABNF resulted in a much prolonged half-life (> 18 h), regardless of the linker length (Fig. 6). Pegylation of Exenatide with 5–40 kDa PEG chains resulted in

	KD (nM)			
	MSA		HSA	
	pH7.4	pH 6	pH 7.4	pH 6
ABNF	25	1	4.5	0.8
Exenatide-4aa-ABNF	21.4	0.67	6.59	0.41
Exenatide-Exenatide-4aa-ABNF	10.65	2.16	5.5	0.96

Fig. 4. KD values in nM of the Exenatide-ABNF fusions at pH 7.4 and 6 on MSA and HSA as measured in Octet Qke.

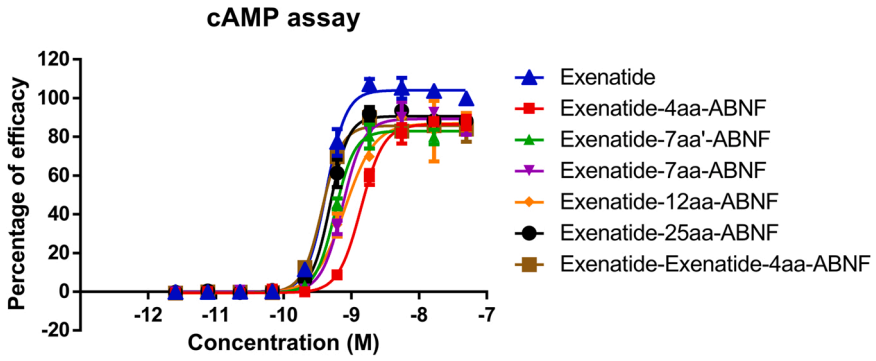

Name	EC50 (nM)
Exenatide	0.4265
Exenatide-4aa-ABNF	1.387
Exenatide-7aa'-ABNF	0.5785
Exenatide-7aa-ABNF	0.7459
Exenatide-12aa-ABNF	0.8065
Exenatide-25aa-ABNF	0.4903
Exenatide-Exenatide-4aa-ABNF	0.3708

Fig. 5. Assessment of the functionality of recombinant Exenatide and Exenatide-ABNF fusions in the classical in vitro GLP1R cell based assay based on cAMP measurements (n = 2).

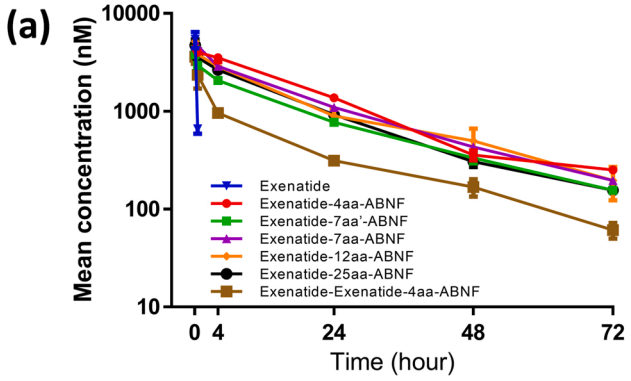

(b)

Pharmacokinetics parameters			
Analytes	Dose (nmol/kg)	CL (mL/h/kg)	$t_{1/2z}$ (h)
Exenatide	1200	610*	0.137*
Exenatide-4aa-ABNF	400	4.02	19.6
Exenatide-7aa'-ABNF	400	6.38	20.8
Exenatide-7aa-ABNF	400	4.62	19.3
Exenatide-12aa-ABNF	400	4.83	21.9
Exenatide-25aa-ABNF	370	5.47	18.7
Exenatide-Exenatide-4aa-ABNF	300	9.87	20.5

*: data estimated

Fig. 6. Quantitative immunological analysis for half-life determination in plasma. (a) Pharmacokinetic profiles of the Exenatide-ABNF fusions over 72 h after a single bolus injection. Blood sampling was performed at 0.083, 0.5, 4, 24, 48 and 72 h after injection. (b) Table summarizing the pharmacokinetic parameters for all the different Exenatide-ABNF fusions such as the terminal half-life (t1/2 z), the clearance (CL) and the dose.

terminal half-life of maximum 12 h in mice [14]. The longer plasma half-life of Exenatide-ABNF fusions compared to Pegylated Exenatide suggests that ABNF-mediated half-life extension is not only mechanical (size increase to limit renal clearance) and benefit from FcRn-mediated recycling as suggested by its ability at targeting the domain II of HSA.

Biological activity and extended pharmacodynamics effects of Exenatide-ABNF fusions were then confirmed in vivo using an oral glucose tolerance test, with the constructions Exenatide-12aa-ABNF and Exenatide-Exenatide-4aa-ABNF. After the first glucose injection, the blood glucose amount is regulated by administration of the Exenatide alone or exenatide-ABNF fusions and compared to the control showing a rapid drop of glucose. At day 2 after another glucose injection, the animals showed a stabilization effect maintained by the two Exenatide-ABNF fusions compared to Exenatide alone, which we can correlate to their longer residence in the blood stream. A third injection of glucose at day 3 resulted in the same observation, highlighting the durable glucose regulation effect of the Exenatide-ABNF fusions. These experiments demonstrated that the increase of half-life promoted by the ABNF fusion can be translated in sustained activity of at least 3 days in mice with a single injection (Fig. 7).

4. Conclusions

One particular interest of the Nanofitin scaffold technology lies in its high modularity allowing its use as a building block that can be assembled by simple genetic fusion to engineer novel drugs exhibiting the desired biological and pharmacological properties. In this study, we demonstrated that the fusion of Exenatide to an albumin binding Nanofitin (ABNF) results in the generation of a long acting GLP1R agonist drug. Exenatide-ABNF fusion displays potent glycemic control and significantly prolonged duration of action (sustained activity for at least 3 days) compared to the parent peptide. The ABNF binds both the human and mouse serum albumins with high affinity both at pH7.4 and 6. In vivo, the ABNF can tightly mobilize circulating serum albumin and benefit from its FcRn-mediated recycling to provide extended residence in the bloodstream (t1/2 up to 20 h in mice). Furthermore, fusion of the ABNF was found to fully maintain the potency of Exenatide in the classical in vitro GLP1R cell based assay based on cAMP measurements, regardless of the linker length. As a comparison, therapeutically approved fusion of a GLP1R agonist analog to albumin (glucagon) showed a hundred fold loss of activity in a similar assay. We also demonstrated CMC compliant features of the ABNF. Owing to the simple and robust nature of the Nanofitin technology, Exenatide-ABNF fusions could be manufactured using cost-effective bacterial fermentation processes, and showed superior stability and homogeneity profiles than the

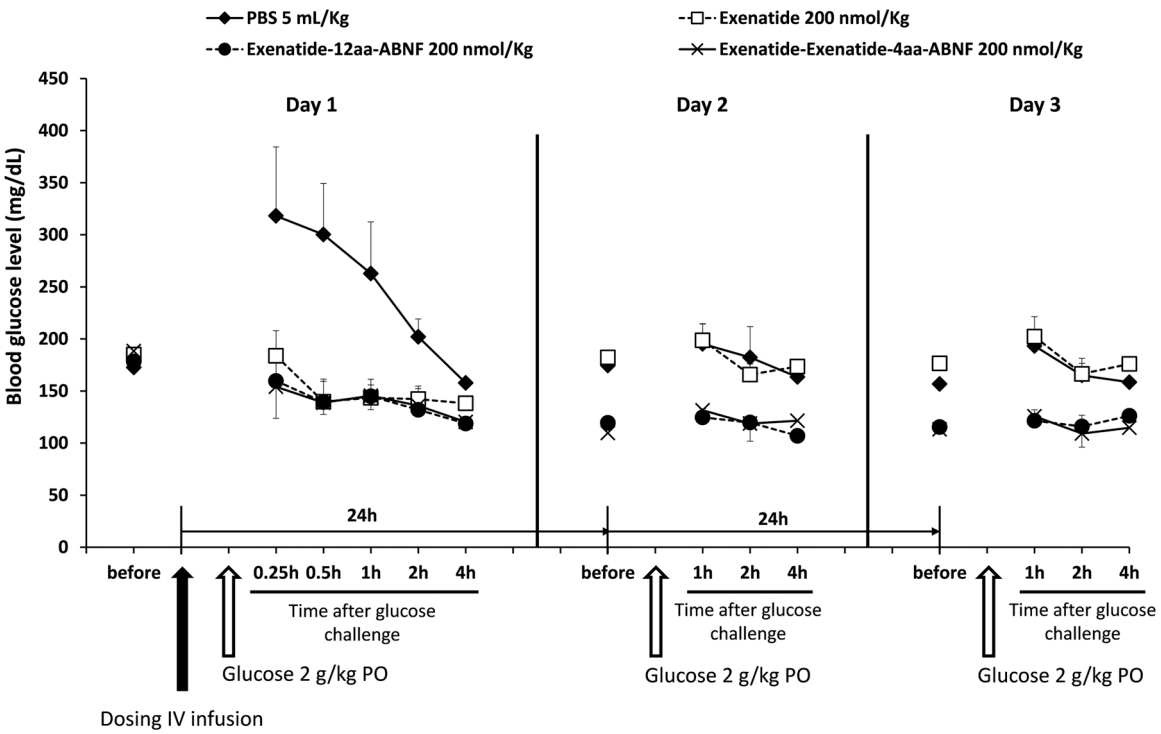

Fig. 7. Oral Glucose Tolerance Test (OGTT). Determination of the potential effect of a single intravenous infusion of 3 fusion proteins: Exenatide, Exenatide-12aa-ABNF and Ex-enatide-Exenatide-4aa-ABNF compared to PBS as a control.

peptide alone.

CRediT authorship contribution statement

Conceptualization, **N.M., J.D., M.C. and O.K.**; methodology, **A.G., N.M., J.D. and M.C.**; validation, **mL.O., MH.P., N.D., J.D. and M.C.**; formal analysis, P.**V., MH.P., A.G., N.D., J.D. and M.C.**; investigation, **A.G., N.M. P.V., MH.P., S.P., P.V. and C.S.**; data curation, **A.G., N.M., C.S. and M.C.**; writing—original draft preparation, **N.M. J.D. and M.C.**; writing—review and editing, **N.M. J.D. and M.C.**; supervision, **J.D., M. C. and O.K.**; project administration, **J.D. and O.K.**; funding acquisition, **J.D.** All authors have read and agreed to the published version of the manuscript.

Declaration of Competing Interest

N. Michot, A. Guyochin, M-H. Pascual, A. Rak, M-L. Ozoux, P. Verdier, P. Vicat and J. Dumas hold employment in Sanofi. M. Cinier, C. Savignard and O. Kitten hold employment in Affilogic. The Nanofitin technology described in this study, commercialized by Affilogic, uses the patent application owned by Institut Pasteur and Centre National de la Recherche Scientifique (CNRS): "OB-fold used as scaffold for engineering new specific binders"; PCT/IB2007/004388.

Acknowledgments

We thank Justine Picot and Anaëlle Perrocheau for their contribution to the generation of the ABNF. We thank Harmony Gorré for her contribution to the characterization of the ABNF. We thank Dr. Simon Huet and Caroline Roze for their contribution to the definition of the HSA domain targeted by the ABNF. We thank Isabelle Coquery and Francis Duffieux for their contribution to the expression of the ABNF and Coralie Werbrouk for her contribution to the purification. We thank Christine Colonna and Anne Severac for their contribution to the ABNF quality control. We thank Thomas Bertrand and Alexey Rak for their contribution to the thermal denaturation. We thank Jean-Dominique Guitton who sponsor the project. We thank Mélanie Roy who performed the biological assays of the dosed animal samples.

Appendix A. Supporting information

Supplementary data associated with this article can be found in the online version at doi:10.1016/j.peptides.2022.170760.

References

[1] P. Caliceti, F.M. Veronese, Pharmacokinetic and biodistribution properties of poly (ethylene glycol)-protein conjugates, Adv. Drug Deliv. Rev. 55 (2003) 1261–1277, https://doi.org/10.1016/s0169-409x(03)00108-x.
[2] S. Jevsevar, M. Kunstelj, V.G. Porekar, PEGylation of therapeutic proteins, Biotechnol. J. 5 (2010) 113–128, https://doi.org/10.1002/biot.200900218.
[3] V.N. Podust, B.-C. Sim, D. Kothari, L. Henthorn, C. Gu, C. Wang, B. McLaughlin, V. Schellenberger, Extension of in vivo half-life of biologically active peptides via chemical conjugation to XTEN protein polymer, Protein Eng. Des. Sel. 26 (2013) 743–753, https://doi.org/10.1093/protein/gzt048.
[4] V.N. Podust, S. Balan, B.-C. Sim, M.P. Coyle, U. Ernst, R.T. Peters, V. Schellenberger, Extension of in vivo half-life of biologically active molecules by XTEN protein polymers. J. Control. Release. 240 (2016) 52–66, https://doi.org/10.1016/j.jconrel.2015.10.038.
[5] J.L. Karnell, M. Albulescu, S. Drabic, L. Wang, R. Moate, M. Baca, V. Oganesyan, M. Gunsior, T. Thisted, L. Yan, J. Li, X. Xiong, S.C. Eck, M. de Los Reyes, I. Yusuf, K. Streicher, U. Muller-Ladner, D. Howe, R. Ettinger, R. Herbst, J. Drappa, A CD40L-targeting protein reduces autoantibodies and improves disease activity in patients with autoimmunity, Sci. Transl. Med. 11 (2019), https://doi.org/10.1126/scitranslmed.aar6584.
[6] A. Jonsson, J. Dogan, N. Herne, L. Abrahmsen, P.-A. Nygren, Engineering of a femtomolar affinity binding protein to human serum albumin, Protein Eng. Des. Sel. 21 (2008) 515–527, https://doi.org/10.1093/protein/gzn028.
[7] D. Sleep, J. Cameron, L.R. Evans, Albumin as a versatile platform for drug half-life extension, Biochim. Biophys. Acta 1830 (2013) 5526–5534, https://doi.org/10.1016/j.bbagen.2013.04.023.
[8] J. Eng, W.A. Kleinman, L. Singh, G. Singh, J.P. Raufman, Isolation and characterization of exendin-4, an exendin-3 analogue, from Heloderma suspectum venom. Further evidence for an exendin receptor on dispersed acini from guinea pig pancreas, J. Biol. Chem. 267 (1992) 7402–7405.
[9] P.L. McCormack, Exenatide twice daily: a review of its use in the management of patients with type 2 diabetes mellitus, Drugs 74 (2014) 325–351, https://doi.org/10.1007/s40265-013-0172-6.
[10] M. Lorenz, A. Evers, M. Wagner, Recent progress and future options in the development of GLP-1 receptor agonists for the treatment of diabesity, Bioorg.

Med. Chem. Lett. 23 (2013) 4011–4018, https://doi.org/10.1016/j.bmcl.2013.05.022.
[11] Y. Cai, L. Wei, L. Ma, X. Huang, A. Tao, Z. Liu, W. Yuan, Long-acting preparations of exenatide. Drug Des. Devel. Ther. 7 (2013) 963–970, https://doi.org/10.2147/DDDT.S46970.
[12] W. Bao, L.J. Holt, R.D. Prince, G.X. Jones, K. Aravindhan, M. Szapacs, A. M. Barbour, L.J. Jolivette, J.J. Lepore, R.N. Willette, E. DeAngelis, B.M. Jucker, Novel fusion of GLP-1 with a domain antibody to serum albumin prolongs protection against myocardial ischemia/reperfusion injury in the rat, Cardiovasc. Diabetol. 12 (2013) 148, https://doi.org/10.1186/1475-2840-12-148.
[13] L.L. Baggio, Q. Huang, T.J. Brown, D.J. Drucker, A recombinant human glucagon-like peptide (GLP)-1-albumin protein (albugon) mimics peptidergic activation of GLP-1 receptor-dependent pathways coupled with satiety, gastrointestinal motility, and glucose homeostasis, Diabetes 53 (2004) 2492–2500, https://doi.org/10.2337/diabetes.53.9.2492.
[14] N. Gong, A.-N. Ma, L.-J. Zhang, X.-S. Luo, Y.-H. Zhang, M. Xu, Y.-X. Wang, Site-specific PEGylation of exenatide analogues markedly improved their glucoregulatory activity, Br. J. Pharmacol. 163 (2011) 399–412, https://doi.org/10.1111/j.1476-5381.2011.01227.x.
[15] F. Selis, R. Schrepfer, R. Sanna, S. Scaramuzza, G. Tonon, S. Dedoni, P. Onali, G. Orsini, S. Genovese, Enzymatic mono-pegylation of glucagon-like peptide 1 towards long lasting treatment of type 2 diabetes, Results Pharma Sci 2 (2012) 58–65, https://doi.org/10.1016/j.rinphs.2012.09.001.
[16] V. Schellenberger, C.-W. Wang, N.C. Geething, B.J. Spink, A. Campbell, W. To, M. D. Scholle, Y. Yin, Y. Yao, O. Bogin, J.L. Cleland, J. Silverman, W.P.C. Stemmer, A recombinant polypeptide extends the in vivo half-life of peptides and proteins in a tunable manner, Nat. Biotechnol. 27 (2009) 1186–1190, https://doi.org/10.1038/nbt.1588.
[17] A. Zorzi, S. Linciano, A. Angelini, Non-covalent albumin-binding ligands for extending the circulating half-life of small biotherapeutics, Medchemcomm 10 (2019) 1068–1081, https://doi.org/10.1039/c9md00018f.
[18] D. Kim, H. Jeon, S. Ahn, W. Il Choi, S. Kim, S. Jon, An approach for half-life extension and activity preservation of an anti-diabetic peptide drug based on genetic fusion with an albumin-binding aptide. J. Control. Release. 256 (2017) 114–120, https://doi.org/10.1016/j.jconrel.2017.04.036.
[19] H. Robinson, Y.G. Gao, B.S. McCrary, S.P. Edmondson, J.W. Shriver, A.H. Wang, The hyperthermophile chromosomal protein Sac7d sharply kinks DNA, Nature 392 (1998) 202–205, https://doi.org/10.1038/32455.
[20] B. Mouratou, F. Schaeffer, I. Guilvout, D. Tello-Manigne, A.P. Pugsley, P.M. Alzari, F. Pecorari, Remodeling a DNA-binding protein as a specific in vivo inhibitor of bacterial secretin PulD., Proc. Natl. Acad. Sci. U. S. A. 104 (2007) 17983–17988. ⟨https://doi.org/10.1073/pnas.0702963104⟩.
[21] G. Behar, M. Bellinzoni, M. Maillasson, L. Paillard-Laurance, P.M. Alzari, X. He, B. Mouratou, F. Pecorari, Tolerance of the archaeal Sac7d scaffold protein to alternative library designs: characterization of anti-immunoglobulin G Affitins, Protein Eng. Des. Sel. 26 (2013) 267–275, https://doi.org/10.1093/protein/gzs106.
[22] G. Behar, S. Pacheco, M. Maillasson, B. Mouratou, F. Pecorari, Switching an anti-IgG binding site between archaeal extremophilic proteins results in Affitins with enhanced pH stability. J. Biotechnol. 192 (Pt A) (2014) 123–129, https://doi.org/10.1016/j.jbiotec.2014.10.006.
[23] G. Behar, A. Renodon-Corniere, B. Mouratou, F. Pecorari, Affitins as robust tailored reagents for affinity chromatography purification of antibodies and non-immunoglobulin proteins. J. Chromatogr. A. 1441 (2016) 44–51, https://doi.org/10.1016/j.chroma.2016.02.068.
[24] M. Cinier, M. Petit, F. Pecorari, D.R. Talham, B. Bujoli, C. Tellier, Engineering of a phosphorylatable tag for specific protein binding on zirconium phosphonate based microarrays, J. Biol. Inorg. Chem. 17 (2012) 399–407, https://doi.org/10.1007/s00775-011-0863-y.
[25] N. Gera, M. Hussain, R.C. Wright, B.M. Rao, Highly stable binding proteins derived from the hyperthermophilic Sso7d Scaffold, J. Mol. Biol. 409 (2011) 601–616. ⟨http://www.sciencedirect.com/science/article/pii/S0022283611004359⟩.
[26] S. Huet, H. Gorre, A. Perrocheau, J. Picot, M. Cinier, Use of the nanofitin alternative scaffold as a GFP-Ready fusion tag, PLoS One 10 (2015), e0142304, https://doi.org/10.1371/journal.pone.0142304.
[27] V. Kalichuk, G. Behar, A. Renodon-Corniere, G. Danovski, G. Obal, J. Barbet, B. Mouratou, F. Pecorari, The archaeal "7 kDa DNA-binding" proteins: extended characterization of an old gifted family, Sci. Rep. 6 (2016) 37274, https://doi.org/10.1038/srep37274.
[28] V. Kalichuk, A. Renodon-Corniere, G. Behar, F. Carrion, G. Obal, M. Maillasson, B. Mouratou, V. Preat, F. Pecorari, A novel, smaller scaffold for Affitins: Showcase with binders specific for EpCAM, Biotechnol. Bioeng. 115 (2017) 290–299, https://doi.org/10.1002/bit.26463.
[29] B. Mouratou, G. Béhar, L. Paillard-Laurance, S. Colinet, F. Pecorari, Ribosome display for the selection of Sac7d scaffolds, in: Methods, 2012: pp. 191–212. ⟨https://doi.org/10.1007/978–1-61779–379-0⟩.
[30] M. Dockal, D.C. Carter, F. Rüker, The three recombinant domains of human serum albumin. Structural characterization and ligand binding properties, J. Biol. Chem 274 (1999) 29303–29310, https://doi.org/10.1074/jbc.274.41.29303.
[31] S.A. Jacobs, A.C. Gibbs, M. Conk, F. Yi, D. Maguire, C. Kane, K.T. O'Neil, Fusion to a highly stable consensus albumin binding domain allows for tunable pharmacokinetics, Protein Eng. Des. Sel. 28 (2015) 385–393, https://doi.org/10.1093/protein/gzv040.
[32] J. Nilvebrant, S. Hober, The albumin-binding domain as a scaffold for protein engineering. Comput. Struct. Biotechnol. J. 6 (2013), e201303009 https://doi.org/10.5936/csbj.201303009.
[33] R. Stork, E. Campigna, B. Robert, D. Muller, R.E. Kontermann, Biodistribution of a bispecific single-chain diabody and its half-life extended derivatives, J. Biol. Chem. 284 (2009) 25612–25619, https://doi.org/10.1074/jbc.M109.027078.
[34] D. Gefel, G.K. Hendrick, S. Mojsov, J. Habener, G.C. Weir, Glucagon-like peptide-I analogs: effects on insulin secretion and adenosine 3',5'-monophosphate formation, Endocrinology 126 (1990) 2164–2168, https://doi.org/10.1210/endo-126-4-2164.
[35] R.B. Kapust, J. Tozser, T.D. Copeland, D.S. Waugh, The P1' specificity of tobacco etch virus protease, Biochem. Biophys. Res. Commun. 294 (2002) 949–955, https://doi.org/10.1016/S0006-291X(02)00574-0.
[36] M. Bak, J. Park, K. Min, J. Cho, J. Seong, Y.S. Hahn, G. Tae, I. Kwon, Recombinant peptide production platform coupled with site-specific albumin conjugation enables a convenient production of long-acting therapeutic peptide, Pharmaceutics 12 (2020), https://doi.org/10.3390/pharmaceutics12040364.
[37] C. Wu, H. Ying, C. Grinnell, S. Bryant, R. Miller, A. Clabbers, S. Bose, D. McCarthy, R.-R. Zhu, L. Santora, R. Davis-Taber, Y. Kunes, E. Fung, A. Schwartz, P. Sakorafas, J. Gu, E. Tarcsa, A. Murtaza, T. Ghayur, Simultaneous targeting of multiple disease mediators by a dual-variable-domain immunoglobulin, Nat. Biotechnol. 25 (2007) 1290–1297, https://doi.org/10.1038/nbt1345.
[38] X. Chen, J.L. Zaro, W.-C. Shen, Fusion protein linkers: property, design and functionality, Adv. Drug Deliv. Rev. 65 (2013) 1357–1369, https://doi.org/10.1016/j.addr.2012.09.039.
[39] S. Madsbad, Review of head-to-head comparisons of glucagon-like peptide-1 receptor agonists, Diabetes. Obes. Metab. 18 (2016) 317–332, https://doi.org/10.1111/dom.12596.
[40] S. Kubetzko, C.A. Sarkar, A. Pluckthun, Protein PEGylation decreases observed target association rates via a dual blocking mechanism, Mol. Pharmacol. 68 (2005) 1439–1454, https://doi.org/10.1124/mol.105.014910.
[41] F. Brandl, H. Merten, M. Zimmermann, M. Behe, U. Zangemeister-Wittke, A. Pluckthun, Influence of size and charge of unstructured polypeptides on pharmacokinetics and biodistribution of targeted fusion proteins. J. Control. Release. 307 (2019) 379–392, https://doi.org/10.1016/j.jconrel.2019.06.030.
[42] H. Hui, X. Zhao, R. Perfetti, Structure and function studies of glucagon-like peptide-1 (GLP-1): the designing of a novel pharmacological agent for the treatment of diabetes, Diabetes. Metab. Res. Rev. 21 (2005) 313–331, https://doi.org/10.1002/dmrr.553.
[43] O.E. Levy, C.M. Jodka, S.S. Ren, L. Mamedova, A. Sharma, M. Samant, L. J. D'Souza, C.J. Soares, D.R. Yuskin, L.J. Jin, D.G. Parkes, K. Tatarkiewicz, S. S. Ghosh, Novel exenatide analogs with peptidic albumin binding domains: potent anti-diabetic agents with extended duration of action, PLoS One 9 (2014), e87704, https://doi.org/10.1371/journal.pone.0087704.
[44] T.Y. Kim, J.H. Park, H.E. Shim, D.S. Choi, D.-E. Lee, J.-J. Song, H.-S. Kim, Prolonged half-life of small-sized therapeutic protein using serum albumin-specific protein binder. J. Control. Release. 315 (2019) 31–39, https://doi.org/10.1016/j.jconrel.2019.09.017.